Supporting Information

$La_{0.2}Sr_{0.25}Ca_{0.45}TiO_3$ surface reactivity with H_2: a combined *operando* NEXAFS and computational study

Authors: F. Bassato*[1,2], S. Mauri*[1], L. Braglia[1], A. Yu. Petrov[1], E. Dobovičnik[3], F. Tavani[4], A. Tofoni[4], P. Ferrer[5], D. Grinter[5], G. Held[5], P. D'Angelo[4] and P. Torelli*[1]

Affiliations

[1]Istituto Officina dei Materiali IOM–CNR, Laboratorio TASC, Area Science Park, S.S.14, km 163.5, Trieste I-34149, Italy

[2]Department of Physics, University of Trieste, Via A. Valerio 2, Trieste 34127, Italy

[3]Department of Engineering and Architecture, University of Trieste, Via A. Valerio 6/1, Trieste 34127, Italy

[4]Department of Chemistry, University of Rome "La Sapienza", P.le A. Moro 5, 00185 Rome, Italy

[5]Diamond Light Source, Oxfordshire OX11 0DE, U.K.

Corresponding Authors

Ferdinando Bassato – *Istituto Officina dei Materiali IOM-CNR, Laboratorio TASC*, Trieste I-34149*; Department of Physics, University of Trieste, 34127 Trieste, Italy;* Email: bassato@iom.cnr.it

Silvia Mauri – *Istituto Officina dei Materiali IOM-CNR, Laboratorio TASC*, Trieste I-34149; Email: mauri@iom.cnr.it

Piero Torelli – *Istituto Officina dei Materiali IOM-CNR, Laboratorio TASC*, Trieste I-34149; Email: torelli@iom.cnr.it

XRD Patterns

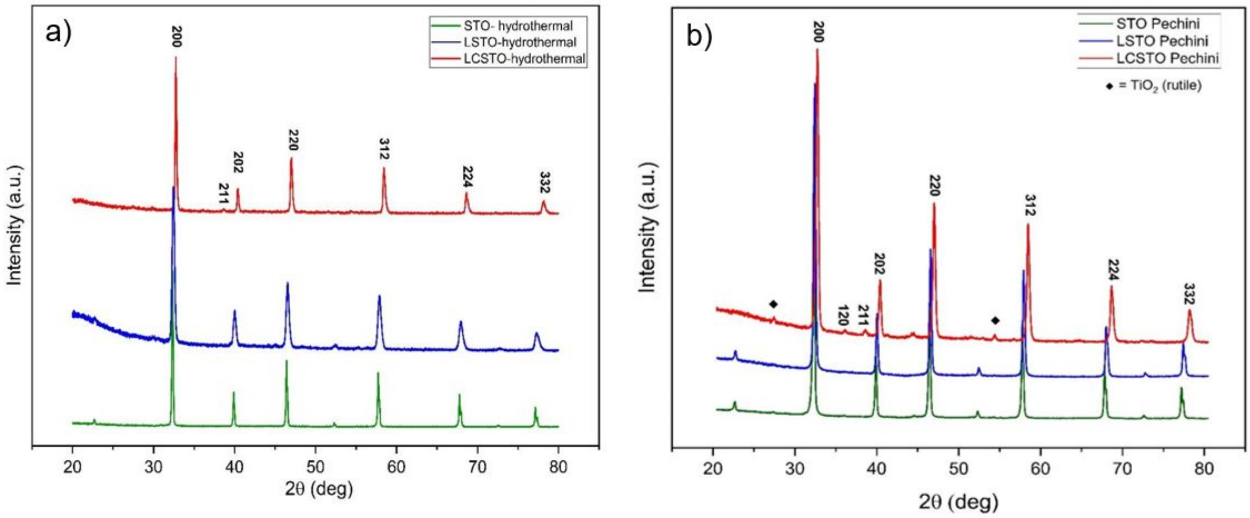

Fig. S1 XRD pattern of the samples synthesized by hydrothermal route (a) and modified-Pechini (b)

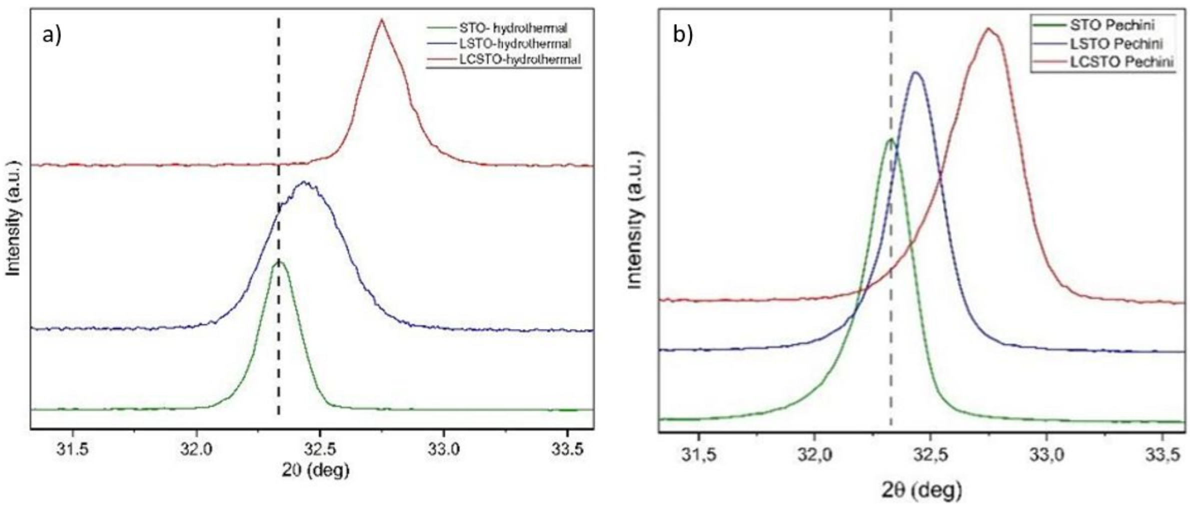

Fig. S2 Inset on the (200) reflection of figure S1

	LCSTO Hydrothermal	LCSTO Pechini
a (Å)	5.5419	5.5432
b (Å)	5.4974	5.4937
c (Å)	7.7995	7.7966

Table S1: LCSTO cell parameters calculated from XRD

Particle size analysis

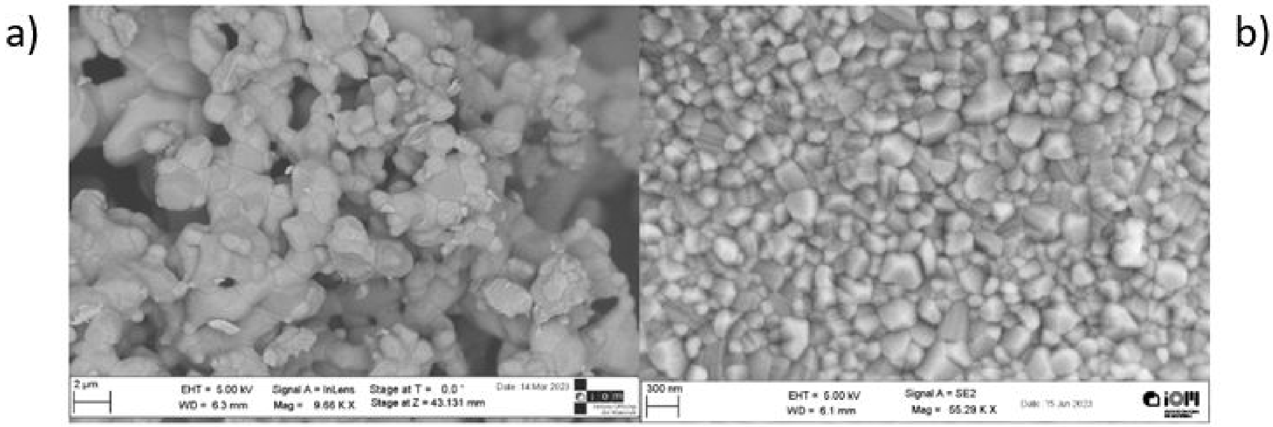

Fig. S3 SEM images of LCSTO Hydrothermal (a) and LCSTO Pechini (b)

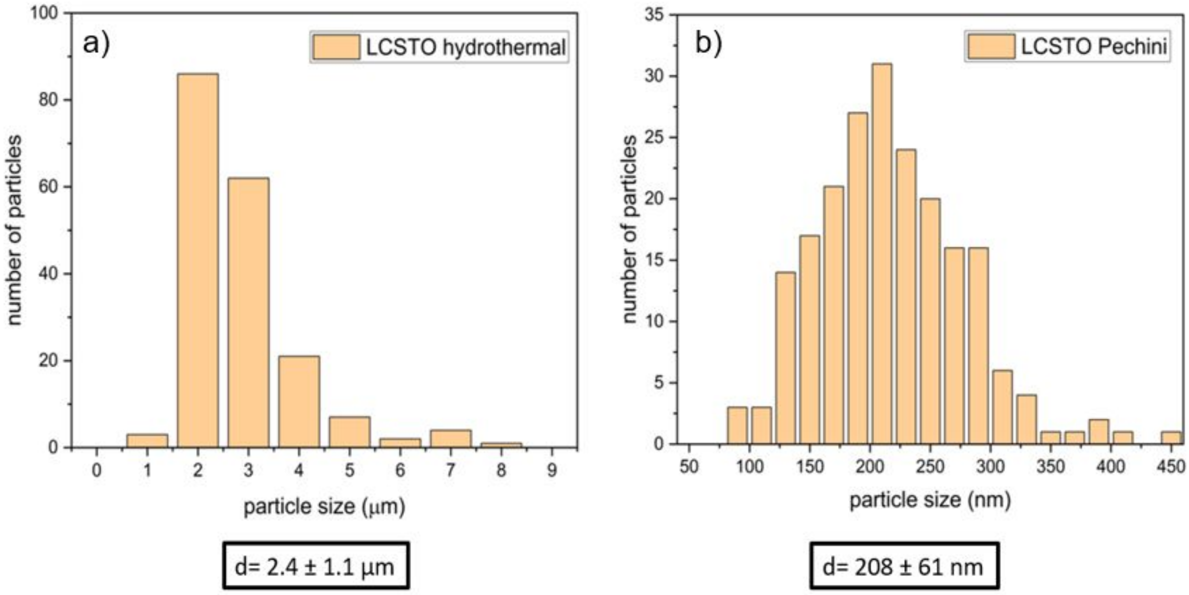

Fig. S4 Size distribution of LCSTO hydrothermal (a) and LCSTO Pechini (b)

XPS Surveys

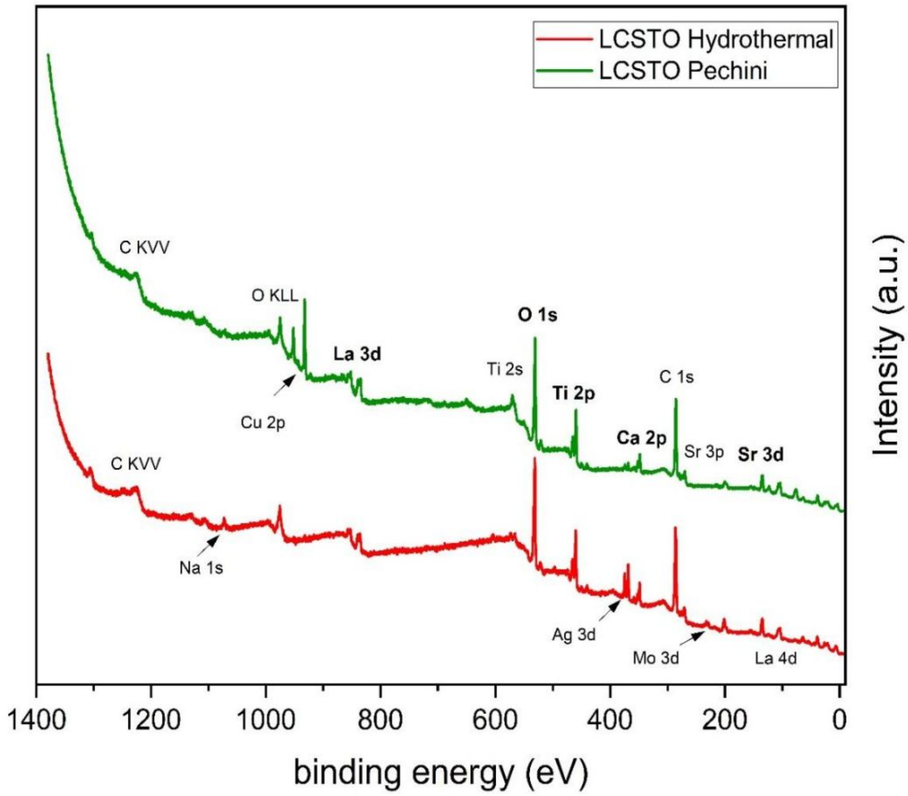

Fig. S5 Surveys of LCSTO samples (Cu and Mo peaks are ascribed to the sample holders, while Ag to silver paint)

XPS core levels fittings

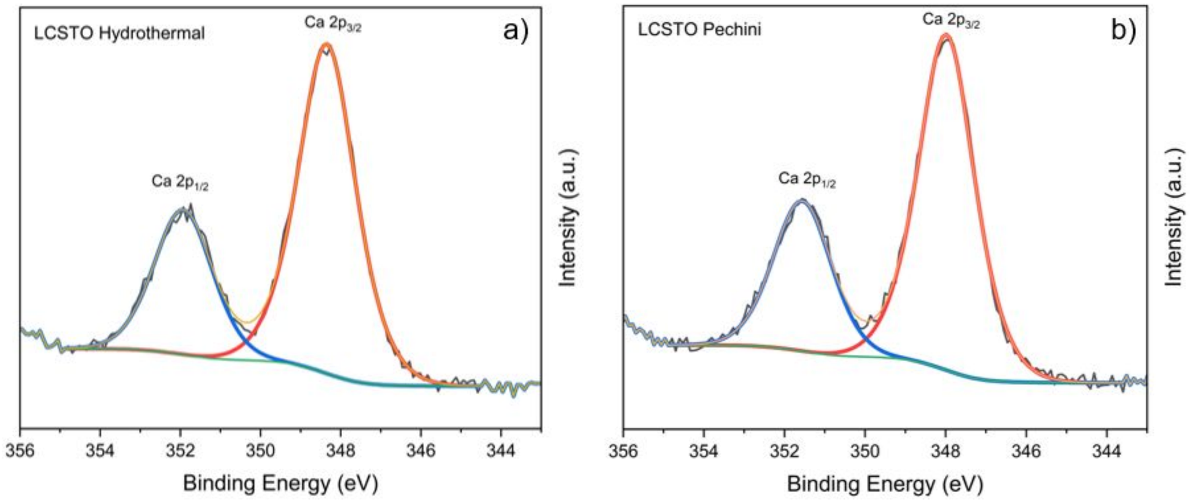

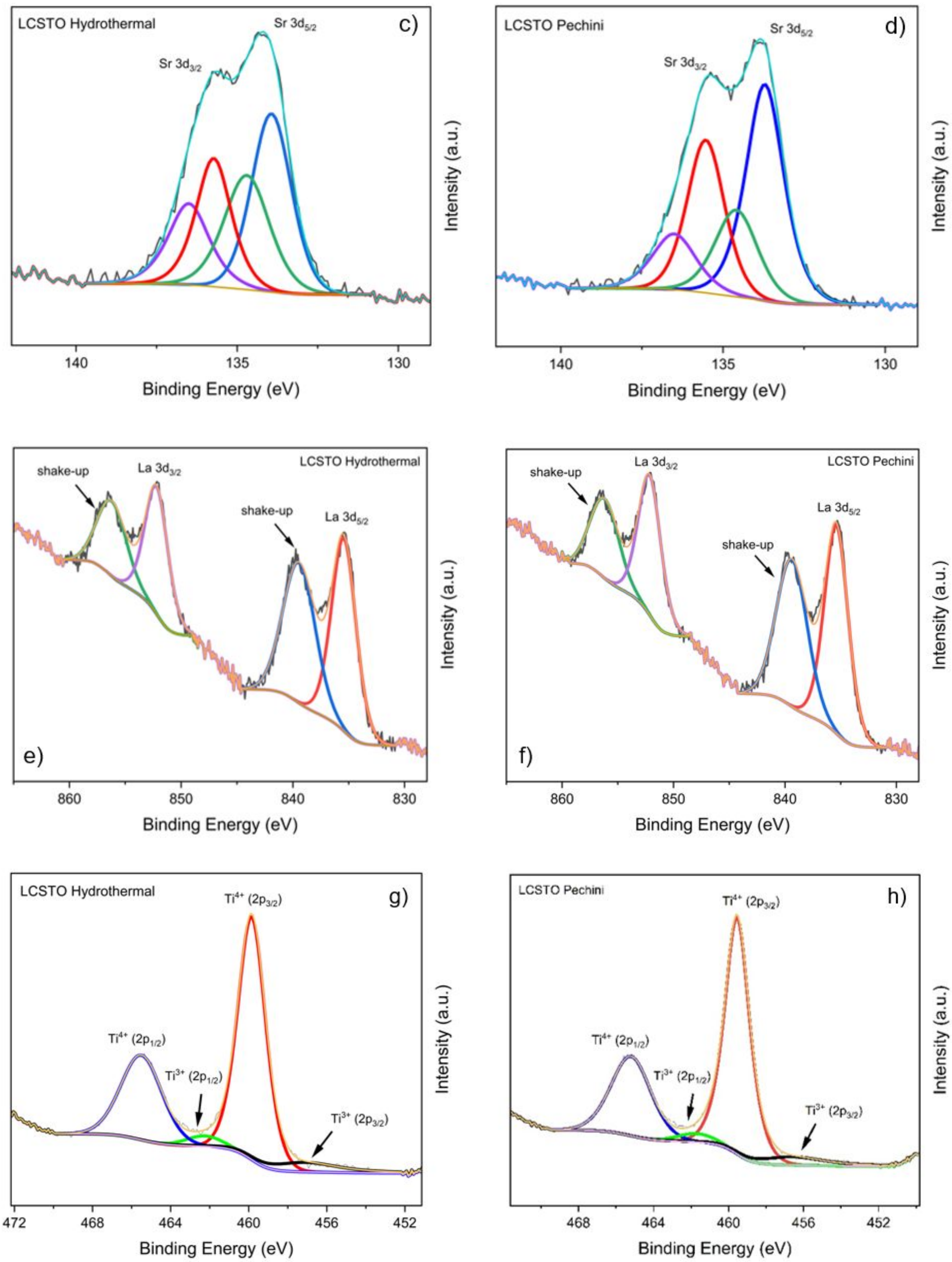
LCSTO Hydrothermal
c)
Sr 3d5/2
Sr 3d3/2
Intensity (a.u.)
140
135
130
Binding Energy (eV)
LCSTO Pechini
d)
Sr 3d5/2
Sr 3d3/2
Intensity (a.u.)
140
135
130
Binding Energy (eV)
shake-up
La 3d3/2
LCSTO Hydrothermal
shake-up
La 3d5/2
Intensity (a.u.)
e)
860
850
840
830
Binding Energy (eV)
shake-up
La 3d3/2
LCSTO Pechini
La 3d5/2
shake-up
Intensity (a.u.)
f)
860
850
840
830
Binding Energy (eV)
LCSTO Hydrothermal
Ti4+ (2p3/2)
g)
Ti4+ (2p1/2)
Ti3+ (2p1/2)
Ti3+ (2p3/2)
Intensity (a.u.)
472
468
464
460
456
452
Binding Energy (eV)
LCSTO Pechini
Ti4+ (2p3/2)
h)
Ti4+ (2p1/2)
Ti3+ (2p1/2)
Ti3+ (2p3/2)
Intensity (a.u.)
468
464
460
456
452
Binding Energy (eV)

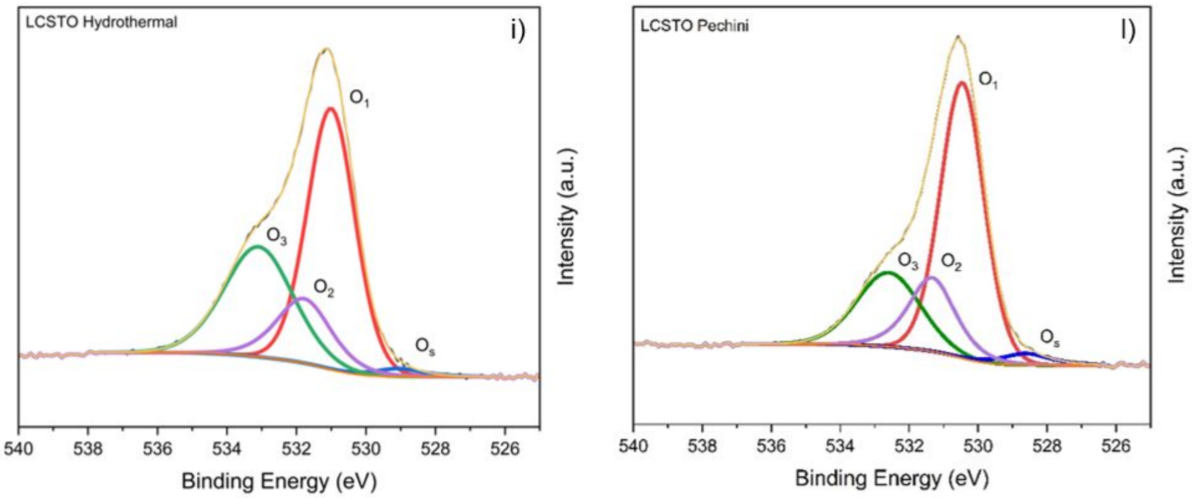

Fig. S6 XPS core levels fittings for LCSTO Hydrothermal and Pechini

O1s LCSTO Hydrothermal					
	Position	FWHM	Line shape	Area	relative %
Lattice (O_1)	531.0 eV	1.61 eV	GL (30)	92521.3	51.34
Vacancies (O_2)	531.78 eV	1.86 eV	GL (60)	27610.7	15.32
-OH (O_3)	533.09 eV	2.33 eV	GL (40)	56990.3	31.62
Sample holder (O_S)	529.06 eV	1.61 eV	GL (80)	3103.9	1.72
Residual STD= 1.048					

Table S2: XPS fitting parameters for O1s: sample LCSTO Hydrothermal

O1s LCSTO Pechini					
	Position	FWHM	Line shape	Area	relative %
Lattice (O_1)	530.46 eV	1.48 eV	GL (30)	74316.6	57.20
Vacancies (O_2)	531.33 eV	1.59 eV	GL (70)	22813.1	17.56
-OH (O_3)	532.59 eV	2.15 eV	GL (30)	29074	22.38
Sample holder (O_S)	528.61 eV	1.64 eV	GL (80)	3711.9	2.86
Residual STD= 1.238					

Table S3: XPS fitting parameters for O1s: sample LCSTO Pechini

SAMPLE	Theoretical Stoichiometry	XPS outcome
LCSTO-Hydrothermal	$La_{0.2}Sr_{0.25}Ca_{0.45}TiO_3$	$La_{0.20}Sr_{0.40}Ca_{0.50}TiO_3$
LCSTO-Pechini	"	$La_{0.20}Sr_{0.40}Ca_{0.50}TiO_3$
LCSTO-MBE pristine	"	$La_{0.15}Sr_{0.40}Ca_{0.40}TiO_3$
LCSTO-MBE "spent"	"	$La_{0.30}Sr_{0.70}Ca_{0.50}TiO_3$

Table S4: LCSTO estimated stoichiometry by XPS

Experimental procedure for the *Operando* NEXAFS experiments

All the samples were subjected to the same experimental procedure: firstly, the sample was pre-heated to 120 °C in pure He flow to remove the adsorbed water and possible contaminants. Then, it was cooled down to RT and heated up to 350 or 400 °C in H_2 (100%). A graphical scheme of the experimental procedure is reported in fig. S7 for clarity.

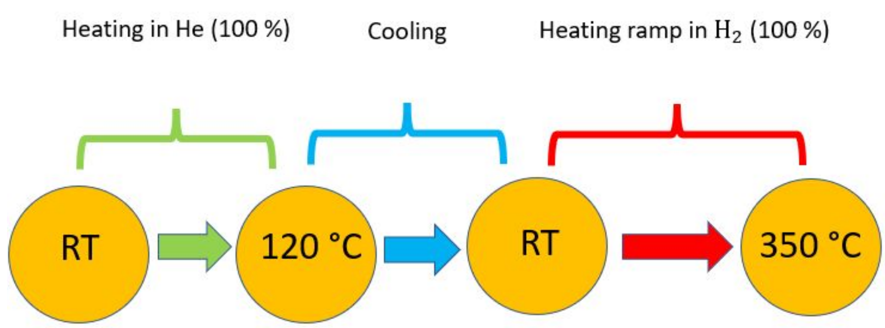

Fig. S7 Experimental scheme of the measurements

Detailed description of STO, LSTO, LCSTO NEXAFS features

Starting the description from lower photon energies, L_3 edge shows two pre-edge peaks (**a** and **b** in Fig. 2)) located at ~ 460.5 and 461.5 eV, assigned to transitions towards virtual orbitals of t_{2g}-like symmetry[1,2], originated from $2p^6\ d^0 \rightarrow 2p^5\ d^1$ transition for Ti^{4+} in O_h symmetry and characteristic of d^0 compounds[3]. The presence of the crystal field in proximity of the octahedral Ti^{4+}sites cause the loss of the 3d orbitals degeneracy, giving rise to the well-known t_{2g} and e_g states: this is reflected by the splitting of the L edges white line. In detail, **c** and **e** structures can be attributed to $2p^{3/2} \rightarrow 3d_{t2g}$ and $2p^{1/2} \rightarrow 3d_{t2g}$ transitions while **d** and **f** to $2p^{3/2} \rightarrow 3d_{eg}$ and $2p^{1/2} \rightarrow 3d_{eg}$. It is important to highlight that, in the presence of O_h symmetry, e_g states are related to dz^2 and dx^2-y^2 orbitals which are strongly hybridized with the ligands (in the case of $SrTiO_3$ with O atoms) because of their geometry. This results in a major sensitivity of the **d** and **f** structures to the Ti-O bonds modifications in the NEXAFS spectra, that could originate from structural distortions or oxygen vacancy formation. Vibronic effects and a larger dispersion caused by a higher degree of hybridization of the Ti 3d e_g orbitals with the surrounding O atoms also reflects in the broadening of **d** and **f**[2,3].

Theoretical Modelling

For $SrTiO_3$, the theoretical spectra have been calculated starting from the corresponding crystallographic structure (*Acta Cryst.* (1995). B**51**, 942-951 https://doi.org/10.1107/S0108768195003752, 10.1103/PhysRevB.60.2961). The .cif file containing the crystallographic parameters was employed to build a $SrTiO_3$ cluster (fig. S8) that was used for the theoretical simulations of the spectra.

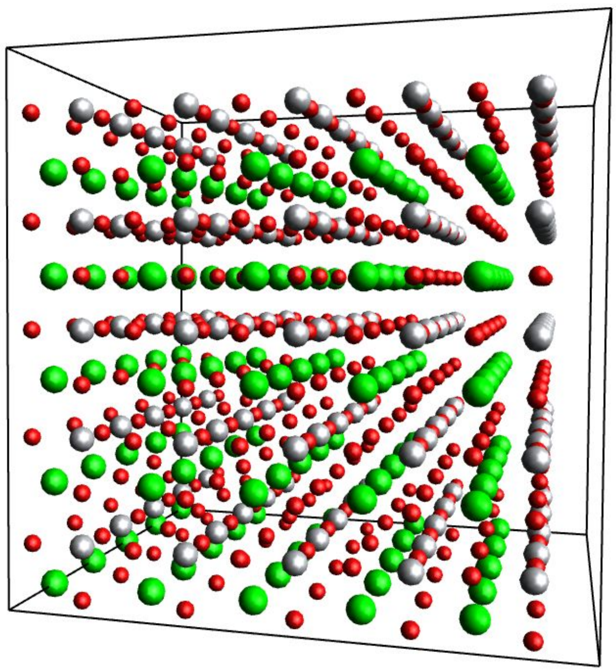

Figure S8. 5x5x5 $SrTiO_3$ supercell model used for the theoretical simulations. The dimensions of the unit cell are a=b=c= 3.908 Å, α=β=γ=90°.

The photoabsorber atom has been chosen in order to be at the centre of the cluster, therefore with crystallographic coordinates x=0, y=0 and z=0. The same procedure has been employed to build analogue clusters with different crystallographic parameters and chemical compositions, described in detail hereafter. In order to build the $La_{0.2}Sr_{0.25}Ca_{0.45}TiO_3$ cluster, the $SrTiO_3$ crystal structure was chosen as a starting point. To have a clear view of the operations carried out on the $SrTiO_3$ structure, a simplified picture of its cubic unit cell is shown in fig. S9, where the first and second coordination shells of the photoabsorber atom are clearly observable (Model 1). In detail, the central Ti site is bound to six oxygen atoms in octahedral coordination, while eight Sr atoms occupy the corners of the resulting FCC cell. In order to build the $La_{0.2}Sr_{0.25}Ca_{0.45}TiO_3$ model, two operations have been performed on the $SrTiO_3$ structure:

- Structural modification: $La_{0.2}Sr_{0.25}Ca_{0.45}TiO_3$ has an orthorhombic unit cell. The cell parameters have been calculated from the XRD patterns (table S1); the values found were then replaced to those of the $SrTiO_3$ structure when building the cluster model. The resulting orthorhombic unit cell is shown in fig. S9 (Model 2).
- Chemical modification: Starting from Model 2 and keeping the same cell parameters, four Sr atoms have been replaced with Ca atoms, while two Sr atoms have been substituted by La atoms (Model 3).

In Model 4, the cubic unit cell of $SrTiO_3$ has been modified, substituting a Sr atom with a La atom. In order to simulate the structural and chemical modifications that occurred after exposing the $La_{0.2}Sr_{0.25}Ca_{0.45}TiO_3$ to H_2 atmosphere, Model 5 was built: it has the same cell parameters of Model 3 with the addition of an oxygen vacancy.

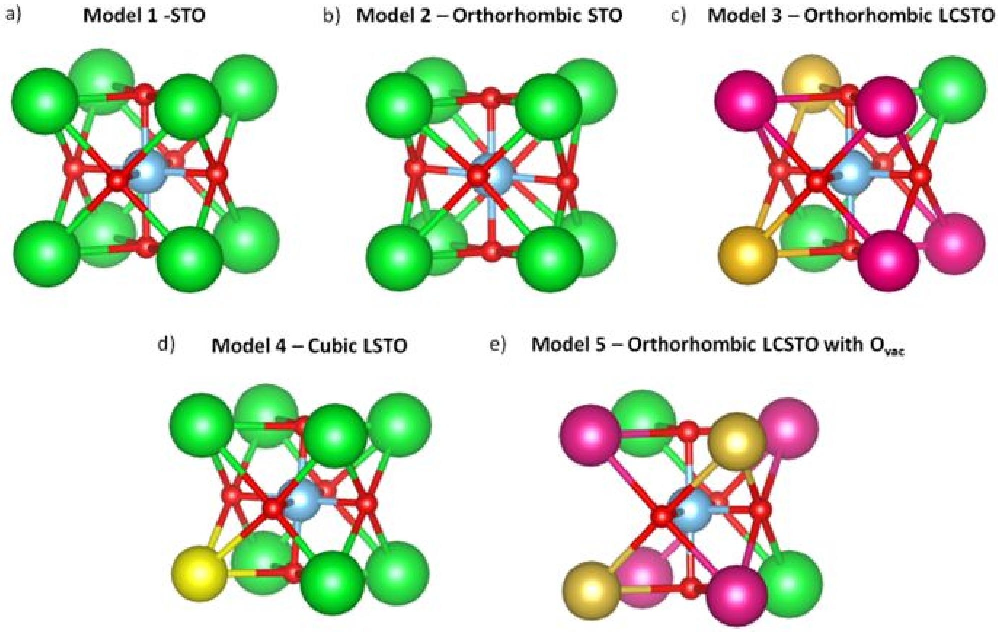

Figure S9 – a) Model 1: Cubic Unit Cell of $SrTiO_3$; b) Model 2: Unit cell of $SrTiO_3$ where cell parameters have been substituted with the ones of $La_{0.2}Sr_{0.25}Ca_{0.45}TiO_3$, resulting in an orthorhombic unit cell; c) Model 3: Orthorhombic Unit cell used to simulate the structure of $La_{0.2}Sr_{0.25}Ca_{0.45}TiO_3$. d) Model 4: Cubic unit cell of $SrTiO_3$ where one Sr atom has been substituted by a La atom. e) Model 5: Orthorhombic Unit cell used to simulate the structure of $La_{0.2}Sr_{0.25}Ca_{0.45}TiO_3$, with an oxygen vacancy. Green: Strontium; Red: Oxygen; Blue: Titanium; Yellow: Lanthanum; Purple: Calcium.

For model 3, it should be taken into account that La, Ca and Sr atoms can be arranged in different configurations in the first coordination shell of Ti. Considering as a first approximation a cubic unit cell, the number of unique permutations of the vertices is 420. When also symmetry is included, this number reduces to 17 different ways to arrange the atoms. For this reason, we performed separate calculations for the seventeen different configurations when calculating Ti^{4+} and Ti^{3+} L edges of LCSTO: the results are reported in Fig. S10

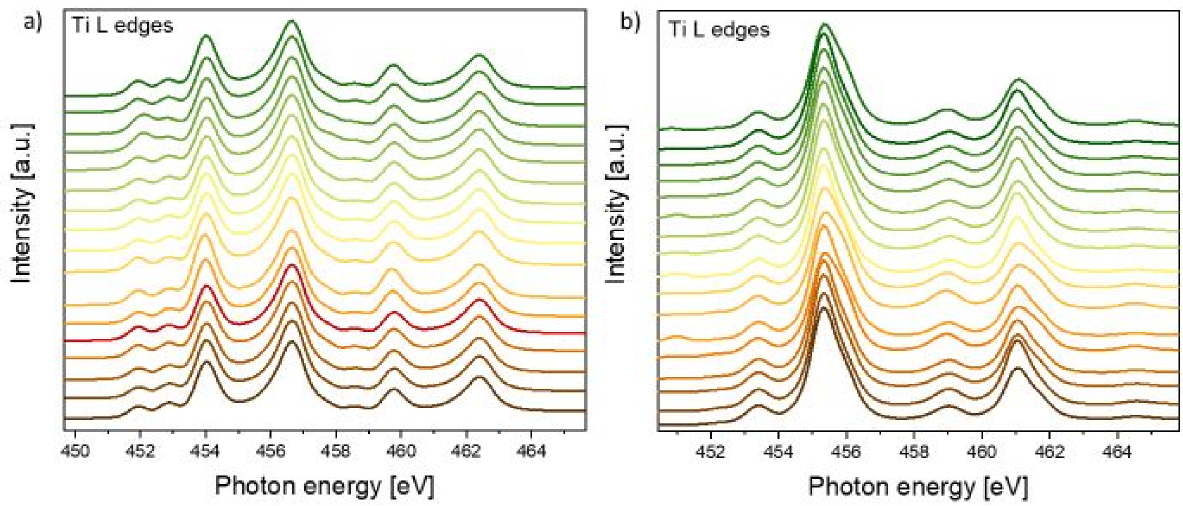

Figure S10 – Ti^{4+} (left) and Ti^{3+}(right) L edges simulations of LCSTO, considering the seventeen different configuration in which La, Ca and Sr can be arranged in model 3.

Fig. S10 shows clearly that the differences detected in the different spectra are almost negligible for the purpose of these simulations: it can be indeed observed that the position and intensity of the main features are very similar. Since the experimental spectra we show in this work are realistically a mean of all the possible configurations, we averaged these simulated spectra to obtain the calculated ones we show in the main manuscript. Clusters analogous to the one of STO have been built for model 2-5, according to their crystallographic cell parameters.

Input structure

As an example, the input structure employed for $SrTiO_3$ is reported hereafter. We highlighted the most important parameters that will be described in the next paragraph. The other keywords used in the input are described in detail in the FDMNES manual (http://www.neel.cnrs.fr/fdmnes, J. Phys. : Condens. Matter 21, 345501 (2009)).

```
Range
-5 .1 10 0.2 20 1 40 2 50

 Energpho
 Edge
  L23
```

```
E_cut
-3.0

Overlap
0.19

 Spinorbite
 Quadrupole
 TDDFT

 Green

 Radius
6.00



Absorber
1

Atom
38 0
22 3 3 2 0 4 0 0 4 1 4
8 2 2 0 2 2 1 4

molecule
1 1 1 90 90 90

2    0.0000000000     0.0000000000     0.0000000000
3   0.0000000000 -1.9495000000    0.0000000000
3   0.0000000000 0.0000000000     -1.9495000000
3   -1.9495000000     0.0000000000     0.0000000000
3   1.9495000000 0.0000000000     0.0000000000
3   0.0000000000 1.9495000000     0.0000000000
3   0.0000000000 0.0000000000     1.9495000000
1   -1.9495000000     -1.9495000000    1.9495000000
```

1	1.9495000000	1.9495000000	-1.9495000000
1	-1.9495000000	1.9495000000	-1.9495000000
1	1.9495000000	1.9495000000	1.9495000000
1	-1.9495000000	1.9495000000	1.9495000000
1	-1.9495000000	-1.9495000000	-1.9495000000
1	1.9495000000	-1.9495000000	-1.9495000000
1	1.9495000000	-1.9495000000	1.9495000000
2	-3.8990000000	0.0000000000	0.0000000000
2	0.0000000000	-3.8990000000	0.0000000000
2	0.0000000000	0.0000000000	-3.8990000000
2	0.0000000000	0.0000000000	3.8990000000
2	0.0000000000	3.8990000000	0.0000000000
2	3.8990000000	0.0000000000	0.0000000000
3	0.0000000000	-3.8990000000	1.9495000000
3	0.0000000000	-1.9495000000	3.8990000000
3	-3.8990000000	1.9495000000	0.0000000000
3	-3.8990000000	0.0000000000	1.9495000000
3	1.9495000000	0.0000000000	-3.8990000000
3	0.0000000000	1.9495000000	-3.8990000000
3	-1.9495000000	0.0000000000	3.8990000000
3	-1.9495000000	3.8990000000	0.0000000000
3	-3.8990000000	0.0000000000	-1.9495000000
3	0.0000000000	-1.9495000000	-3.8990000000
3	0.0000000000	-3.8990000000	-1.9495000000
3	-3.8990000000	-1.9495000000	0.0000000000
3	-1.9495000000	-3.8990000000	0.0000000000
3	1.9495000000	0.0000000000	3.8990000000
3	0.0000000000	1.9495000000	3.8990000000
3	0.0000000000	3.8990000000	-1.9495000000
3	1.9495000000	-3.8990000000	0.0000000000
3	1.9495000000	3.8990000000	0.0000000000
3	0.0000000000	3.8990000000	1.9495000000
3	3.8990000000	-1.9495000000	0.0000000000
3	3.8990000000	0.0000000000	-1.9495000000
3	-1.9495000000	0.0000000000	-3.8990000000
3	3.8990000000	1.9495000000	0.0000000000
3	3.8990000000	0.0000000000	1.9495000000

2	-3.8990000000	3.8990000000	0.0000000000
2	0.0000000000	-3.8990000000	3.8990000000
2	0.0000000000	3.8990000000	3.8990000000
2	3.8990000000	-3.8990000000	0.0000000000
2	-3.8990000000	-3.8990000000	0.0000000000
2	3.8990000000	0.0000000000	-3.8990000000
2	-3.8990000000	0.0000000000	3.8990000000
2	0.0000000000	3.8990000000	-3.8990000000
2	0.0000000000	-3.8990000000	-3.8990000000
2	-3.8990000000	0.0000000000	-3.8990000000
2	3.8990000000	0.0000000000	3.8990000000
2	3.8990000000	3.8990000000	0.0000000000
3	-1.9495000000	3.8990000000	-3.8990000000
3	-3.8990000000	3.8990000000	-1.9495000000
3	0.0000000000	0.0000000000	5.8485000000
3	-3.8990000000	-3.8990000000	-1.9495000000
3	1.9495000000	3.8990000000	-3.8990000000
3	1.9495000000	-3.8990000000	3.8990000000
3	-3.8990000000	-3.8990000000	1.9495000000
3	0.0000000000	0.0000000000	-5.8485000000
3	0.0000000000	5.8485000000	0.0000000000
3	-3.8990000000	3.8990000000	1.9495000000
3	-1.9495000000	3.8990000000	3.8990000000
3	1.9495000000	3.8990000000	3.8990000000
3	3.8990000000	-1.9495000000	-3.8990000000
3	3.8990000000	-3.8990000000	-1.9495000000
3	0.0000000000	-5.8485000000	0.0000000000
3	-1.9495000000	-3.8990000000	3.8990000000
3	3.8990000000	-3.8990000000	1.9495000000
3	3.8990000000	-1.9495000000	3.8990000000
3	-3.8990000000	-1.9495000000	3.8990000000
3	3.8990000000	1.9495000000	-3.8990000000
3	1.9495000000	-3.8990000000	-3.8990000000
3	-5.8485000000	0.0000000000	0.0000000000
3	5.8485000000	0.0000000000	0.0000000000
3	-1.9495000000	-3.8990000000	-3.8990000000
3	-3.8990000000	-1.9495000000	-3.8990000000

```
3    -3.8990000000      1.9495000000      -3.8990000000
3    3.8990000000 1.9495000000      3.8990000000
3    3.8990000000 3.8990000000      -1.9495000000
3    -3.8990000000      1.9495000000      3.8990000000
3    3.8990000000 3.8990000000      1.9495000000
```

Convolution

```
End
```

The electronic configuration of the valence orbitals has been explicitly defined in the input structure, in order to be able to differentiate Ti atoms with different oxidation states. The electronic configuration in the ground state of the valence atoms for Ti^0 is the following:

$3d^2$ $4s^2$ $4p^0$

In order to simulate a Ti photoabsorber with a +4 or +3 oxidation state while keeping the whole cluster neutral, four electrons (two from the 3d and two from the 4s atomic orbitals) and three electrons (one from the 3d and two from the 4s orbitals) were moved to the 4p atomic orbitals, respectively, obtaining the following configurations:

$3d^0$ $4s^0$ $4p^4$ (Ti^{4+})

$3d^1$ $4s^0$ $4p^3$ (Ti^{3+})

For the simulations of $SrTiO_3$ and $LaTiO_3$ compounds, the default convolution parameters of FDMNES code have been adopted (cit manual FDMNES), i.e. using an "arctangent" shape for the broadening. For $La_{0.2}Sr_{0.25}Ca_{0.45}TiO_3$, a Gaussian broadening (FWHM = 0.5) has been employed to better reproduce the experimental spectrum.

Comparison between pre-edge structures of calculated STO and LCSTO NEXAFS spectra

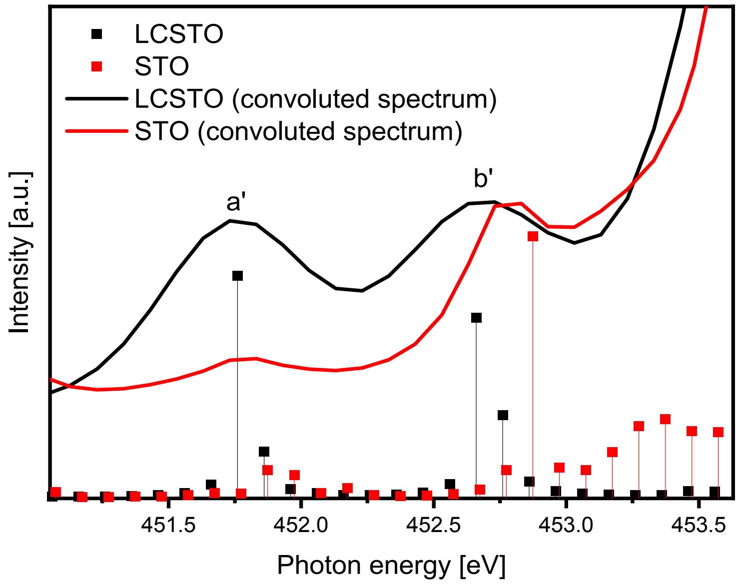

Figure S11 – Pre-edge structures of the calculated spectra of $SrTiO_3$ (red) and $La_{0.2}Sr_{0.25}Ca_{0.45}TiO_3$ (black).

Bars: non convoluted spectra; Solid lines: convoluted spectra.

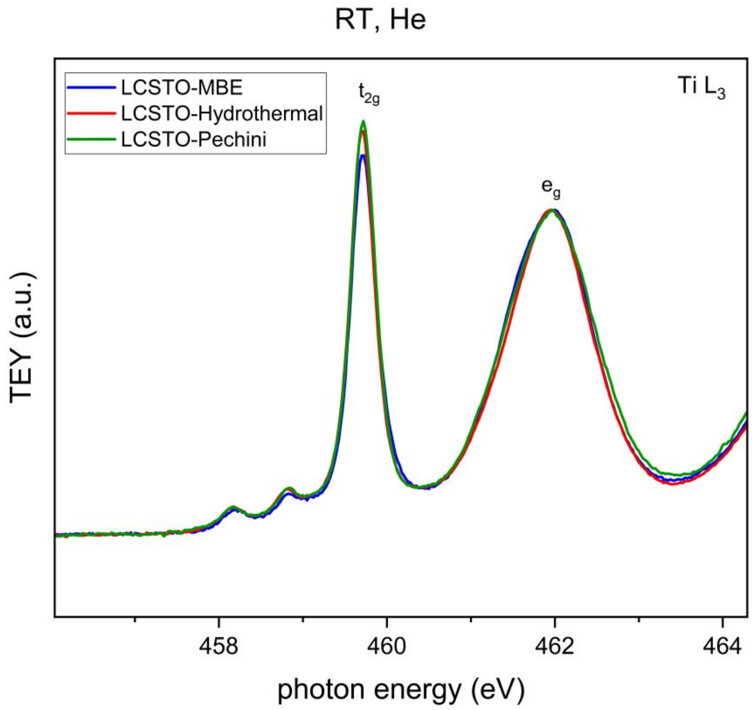

Figure S12 – Ti L_3 edge for LCSTO samples: RT in He

$SrTiO_3$ .cif file

```
# For detailed information please see under Terms & Conditions.

# Full information about CCDC and FIZ Karlsruhe data access policies and
```

```
# citation guidelines are available at http://www.ccdc.cam.ac.uk/access/V1
#
# Audit and citation data items may have been added by FIZ Karlsruhe.
# Please retain this information to preserve the provenance of
# this file and to allow appropriate attribution of the data.
#
#######################################################################

data_80871-ICSD
_database_code_depnum_ccdc_archive 'CCDC 1641048'
loop_
_citation_id
_citation_doi
_citation_year
1 10.1107/S0108768195003752 1995
_audit_update_record
;
2018-02-27 deposited with the CCDC. 2024-01-10 downloaded from the CCDC.
;
_database_code_ICSD                80871
_chemical_name_systematic          'Strontium Titanate'
_chemical_formula_sum              'O3 Sr1 Ti1'
_cell_length_a                     3.8996
_cell_length_b                     3.8996
_cell_length_c                     3.899
_cell_angle_alpha                  90
_cell_angle_beta                   90
_cell_angle_gamma                  90
```

```
_cell_volume                        59.27
_cell_formula_units_Z               1
_symmetry_space_group_name_H-M      'P m -3 m'
_symmetry_Int_Tables_number         221
_symmetry_cell_setting              cubic
_refine_ls_R_factor_all             0.006
loop_
_symmetry_equiv_pos_site_id
_symmetry_equiv_pos_as_xyz
1 'z, y, -x'
2 'y, x, -z'
3 'x, z, -y'
4 'z, x, -y'
5 'y, z, -x'
6 'x, y, -z'
7 'z, -y, x'
8 'y, -x, z'
9 'x, -z, y'
10 'z, -x, y'
11 'y, -z, x'
12 'x, -y, z'
13 '-z, y, x'
14 '-y, x, z'
15 '-x, z, y'
16 '-z, x, y'
17 '-y, z, x'
18 '-x, y, z'
19 '-z, -y, -x'
```

20 '-y, -x, -z'

21 '-x, -z, -y'

22 '-z, -x, -y'

23 '-y, -z, -x'

24 '-x, -y, -z'

25 '-z, -y, x'

26 '-y, -x, z'

27 '-x, -z, y'

28 '-z, -x, y'

29 '-y, -z, x'

30 '-x, -y, z'

31 '-z, y, -x'

32 '-y, x, -z'

33 '-x, z, -y'

34 '-z, x, -y'

35 '-y, z, -x'

36 '-x, y, -z'

37 'z, -y, -x'

38 'y, -x, -z'

39 'x, -z, -y'

40 'z, -x, -y'

41 'y, -z, -x'

42 'x, -y, -z'

43 'z, y, x'

44 'y, x, z'

45 'x, z, y'

46 'z, x, y'

47 'y, z, x'

```
48 'x, y, z'

loop_

_atom_site_label

_atom_site_type_symbol

_atom_site_fract_x

_atom_site_fract_y

_atom_site_fract_z

Sr1 Sr2+ 0 0 0

Ti1 Ti4+ 0.5 0.5 0.5

O1 O2- 0 0.5 0.5


#End of data_80871-ICSD
```

$LaTiO_3$ .cif file

```
#######################################################################

#

# This file contains crystal structure data downloaded from the

# Cambridge Structural Database (CSD) hosted by the Cambridge

# Crystallographic Data Centre (CCDC) in cooperation with FIZ Karlsruhe.

#

# Please note that these data are only for research purposes or private
use.

# For detailed information please see under Terms & Conditions.

# Full information about CCDC and FIZ Karlsruhe data access policies and

# citation guidelines are available at http://www.ccdc.cam.ac.uk/access/V1

#

# Audit and citation data items may have been added by FIZ Karlsruhe.

# Please retain this information to preserve the provenance of

# this file and to allow appropriate attribution of the data.
```

```
#
########################################################################

data_98414-ICSD
_database_code_depnum_ccdc_archive 'CCDC 1657687'
loop_
_citation_id
_citation_doi
_citation_year
1 10.1103/PhysRevB.68.060401 2003
_audit_update_record
;
2018-02-27 deposited with the CCDC. 2022-02-09 downloaded from the CCDC.
;
_database_code_ICSD                98414
_chemical_name_systematic          'Lanthanum Titanate(III)'
_chemical_formula_sum              'La1 O3 Ti1'
_cell_length_a                     5.6336
_cell_length_b                     5.6156
_cell_length_c                     7.9145
_cell_angle_alpha                  90
_cell_angle_beta                   90
_cell_angle_gamma                  90
_cell_volume                       250.38
_cell_formula_units_Z              4
_symmetry_space_group_name_H-M     'P b n m'
_symmetry_Int_Tables_number        62
_symmetry_cell_setting             orthorhombic
```

```
loop_
_symmetry_equiv_pos_site_id
_symmetry_equiv_pos_as_xyz
1 '-x+1/2, y+1/2, z'
2 'x, y, -z+1/2'
3 'x+1/2, -y+1/2, z+1/2'
4 '-x, -y, -z'
5 'x+1/2, -y+1/2, -z'
6 '-x, -y, z+1/2'
7 '-x+1/2, y+1/2, -z+1/2'
8 'x, y, z'
loop_
_atom_site_label
_atom_site_type_symbol
_atom_site_fract_x
_atom_site_fract_y
_atom_site_fract_z
La1 La3+ 0.9916 0.0457 0.25
Ti1 Ti3+ 0.5 0 0
O1 O2- 0.0799 0.4913 0.25
O2 O2- 0.7096 0.2941 0.0417

#End of data_98414-ICSD
```

INPUT STRUCTURE FOR LCSTO

```
Range
-5 .1 10 0.2 20 1 40 2 50
```

```
 Energpho
 Edge
  L23

E_cut
-3.0

Overlap
0.19

 Spinorbite
 Quadrupole
 TDDFT

 Green

 Radius
6.00



Absorber
1

Atom_conf
1 1 3 3 2 0 4 0 0 4 1 4

molecule
1 1 1 90 90 90


 22   0.0000000000   0.0000000000   0.0000000000
  8   0.0000000000  -1.9436000000   0.0000000000
  8   0.0000000000   1.9436000000   0.0000000000
  8  -1.9593500000   0.0000000000   0.0000000000
  8   1.9593500000   0.0000000000   0.0000000000
  8   0.0000000000   0.0000000000  -2.7575350000
```

22	0.0000000000	-3.8872000000	0.0000000000
22	0.0000000000	3.8872000000	0.0000000000
20	-1.9593500000	-1.9436000000	2.7575350000
20	-1.9593500000	-1.9436000000	-2.7575350000
20	-1.9593500000	1.9436000000	2.7575350000
20	1.9593500000	-1.9436000000	-2.7575350000
57	-1.9593500000	1.9436000000	-2.7575350000
57	1.9593500000	-1.9436000000	2.7575350000
38	1.9593500000	1.9436000000	-2.7575350000
38	1.9593500000	1.9436000000	2.7575350000
22	-3.9187000000	0.0000000000	0.0000000000
22	3.9187000000	0.0000000000	0.0000000000
8	-1.9593500000	3.8872000000	0.0000000000
8	-1.9593500000	-3.8872000000	0.0000000000
8	1.9593500000	3.8872000000	0.0000000000
8	1.9593500000	-3.8872000000	0.0000000000
8	3.9187000000	-1.9436000000	0.0000000000
8	3.9187000000	1.9436000000	0.0000000000
8	-3.9187000000	1.9436000000	0.0000000000
8	-3.9187000000	-1.9436000000	0.0000000000
8	0.0000000000	-3.8872000000	2.7575350000
8	0.0000000000	3.8872000000	2.7575350000
8	0.0000000000	3.8872000000	-2.7575350000
8	0.0000000000	-3.8872000000	-2.7575350000
8	3.9187000000	0.0000000000	-2.7575350000
8	-3.9187000000	0.0000000000	2.7575350000
8	-3.9187000000	0.0000000000	-2.7575350000
8	3.9187000000	0.0000000000	2.7575350000
22	0.0000000000	0.0000000000	-5.5150700000
22	0.0000000000	0.0000000000	5.5150700000
22	3.9187000000	3.8872000000	0.0000000000
22	-3.9187000000	3.8872000000	0.0000000000
22	-3.9187000000	-3.8872000000	0.0000000000
22	3.9187000000	-3.8872000000	0.0000000000
8	0.0000000000	-5.8308000000	0.0000000000
8	0.0000000000	5.8308000000	0.0000000000
8	0.0000000000	-1.9436000000	5.5150700000

8	0.0000000000	-1.9436000000	-5.5150700000
8	0.0000000000	1.9436000000	-5.5150700000
8	0.0000000000	1.9436000000	5.5150700000
8	1.9593500000	0.0000000000	-5.5150700000
8	-1.9593500000	0.0000000000	-5.5150700000
8	1.9593500000	0.0000000000	5.5150700000
8	-1.9593500000	0.0000000000	5.5150700000
8	-5.8780500000	0.0000000000	0.0000000000
8	5.8780500000	0.0000000000	0.0000000000
8	3.9187000000	-3.8872000000	-2.7575350000
8	-3.9187000000	-3.8872000000	-2.7575350000
8	3.9187000000	-3.8872000000	2.7575350000
8	3.9187000000	3.8872000000	-2.7575350000
8	-3.9187000000	3.8872000000	-2.7575350000
8	-3.9187000000	3.8872000000	2.7575350000
8	3.9187000000	3.8872000000	2.7575350000
8	-3.9187000000	-3.8872000000	2.7575350000
38	-1.9593500000	5.8308000000	2.7575350000
38	1.9593500000	-5.8308000000	-2.7575350000
38	-1.9593500000	-5.8308000000	-2.7575350000
38	-1.9593500000	5.8308000000	-2.7575350000
38	-1.9593500000	-5.8308000000	2.7575350000
38	1.9593500000	5.8308000000	-2.7575350000
38	1.9593500000	5.8308000000	2.7575350000
38	1.9593500000	-5.8308000000	2.7575350000
22	0.0000000000	-3.8872000000	-5.5150700000
22	0.0000000000	3.8872000000	5.5150700000
22	0.0000000000	-3.8872000000	5.5150700000
22	0.0000000000	3.8872000000	-5.5150700000
22	-3.9187000000	0.0000000000	-5.5150700000
22	3.9187000000	0.0000000000	-5.5150700000
22	-3.9187000000	0.0000000000	5.5150700000
22	3.9187000000	0.0000000000	5.5150700000
38	-5.8780500000	-1.9436000000	-2.7575350000
38	-5.8780500000	-1.9436000000	2.7575350000
38	-5.8780500000	1.9436000000	-2.7575350000
38	5.8780500000	-1.9436000000	-2.7575350000

38	-5.8780500000	1.9436000000	2.7575350000
38	5.8780500000	-1.9436000000	2.7575350000
38	5.8780500000	1.9436000000	-2.7575350000
38	5.8780500000	1.9436000000	2.7575350000
8	-3.9187000000	5.8308000000	0.0000000000
8	3.9187000000	5.8308000000	0.0000000000
8	3.9187000000	-5.8308000000	0.0000000000
8	-3.9187000000	-5.8308000000	0.0000000000
8	1.9593500000	-3.8872000000	5.5150700000
8	-1.9593500000	-3.8872000000	-5.5150700000
8	-1.9593500000	3.8872000000	-5.5150700000
8	1.9593500000	-3.8872000000	-5.5150700000
8	-1.9593500000	3.8872000000	5.5150700000
8	-1.9593500000	-3.8872000000	5.5150700000
8	1.9593500000	3.8872000000	-5.5150700000
8	1.9593500000	3.8872000000	5.5150700000
8	-3.9187000000	-1.9436000000	-5.5150700000
8	3.9187000000	-1.9436000000	5.5150700000
8	-3.9187000000	1.9436000000	5.5150700000
8	3.9187000000	-1.9436000000	-5.5150700000
8	3.9187000000	1.9436000000	-5.5150700000
8	3.9187000000	1.9436000000	5.5150700000
8	-3.9187000000	1.9436000000	-5.5150700000
8	-3.9187000000	-1.9436000000	5.5150700000
8	5.8780500000	-3.8872000000	0.0000000000
8	-5.8780500000	-3.8872000000	0.0000000000
8	5.8780500000	3.8872000000	0.0000000000
8	-5.8780500000	3.8872000000	0.0000000000
22	0.0000000000	7.7744000000	0.0000000000
22	0.0000000000	-7.7744000000	0.0000000000
22	3.9187000000	3.8872000000	-5.5150700000
22	-3.9187000000	3.8872000000	-5.5150700000
22	3.9187000000	3.8872000000	5.5150700000
22	-3.9187000000	-3.8872000000	-5.5150700000
22	3.9187000000	-3.8872000000	5.5150700000
22	-3.9187000000	3.8872000000	5.5150700000
22	-3.9187000000	-3.8872000000	5.5150700000

22	3.9187000000	-3.8872000000	-5.5150700000
22	7.8374000000	0.0000000000	0.0000000000
22	-7.8374000000	0.0000000000	0.0000000000
8	-1.9593500000	-7.7744000000	0.0000000000
8	1.9593500000	-7.7744000000	0.0000000000
8	1.9593500000	7.7744000000	0.0000000000
8	-1.9593500000	7.7744000000	0.0000000000
8	0.0000000000	-5.8308000000	5.5150700000
8	0.0000000000	5.8308000000	5.5150700000
8	0.0000000000	5.8308000000	-5.5150700000
8	0.0000000000	-5.8308000000	-5.5150700000
8	5.8780500000	0.0000000000	5.5150700000
8	-5.8780500000	0.0000000000	-5.5150700000
8	5.8780500000	0.0000000000	-5.5150700000
8	-5.8780500000	0.0000000000	5.5150700000
8	-7.8374000000	-1.9436000000	0.0000000000
8	7.8374000000	1.9436000000	0.0000000000
8	-7.8374000000	1.9436000000	0.0000000000
8	7.8374000000	-1.9436000000	0.0000000000
8	0.0000000000	7.7744000000	-2.7575350000
8	0.0000000000	7.7744000000	2.7575350000
8	0.0000000000	-7.7744000000	2.7575350000
8	0.0000000000	-7.7744000000	-2.7575350000
8	0.0000000000	0.0000000000	-8.2726050000
8	0.0000000000	0.0000000000	8.2726050000
8	-7.8374000000	0.0000000000	-2.7575350000
8	-7.8374000000	0.0000000000	2.7575350000
8	7.8374000000	0.0000000000	2.7575350000
8	7.8374000000	0.0000000000	-2.7575350000

Convolution

Gaussian

0.5

End

- **References**

(1) Yong, Z.; Linghu, J.; Xi, S.; Yin, X.; Leek, M. L.; Shen, L.; Timm, R.; Wee, A. T. S.; Feng, Y. P.; Pan, J. Unravelling Uniaxial Strain Effects on Electronic Correlations, Hybridization and Bonding in Transition Metal Oxides. *Acta Mater* **2019**, *164*, 618–626. https://doi.org/10.1016/j.actamat.2018.11.017.

(2) De Francesco, R.; Stener, M.; Fronzoni, G. Computational Investigation of the L2,3-Edge Spectra of Bulk and (110) Surface of Rutile TiO2. *Surf Sci* **2011**, *605* (5–6), 500–506. https://doi.org/10.1016/j.susc.2010.12.006.

(3) De Groot, F. M. F.; Fuggle, J. C.; Thole, B. T.; Sawatzky, G. A. *L q 3 X-Ray-Absorption Edges of d Compounds: K+, Ca2+, Sc'+, and Ti + in Oh (Octahedral) Symmetry*; 1990; Vol. 8.